Fracture of Scantling Support Structure of Gas Processing Module on FPSO

F. M. Mufti[a], Efi Afrizal[b], E. B. Djatmiko[c], Murdjito[c], Jaswar[b]*

[a]Department of Information, Politeknik Batam, Indonesia
[b]Department of Aeronautic, Automotive and Ocean Engineering, Faculty of Mechanical Engineering, Universiti Teknologi Malaysia, 81310 UTM Johor Bahru, Johor, Malaysia
[c]Department of Ocean Engineering, Faculty of Marine Technology, Institut Technologi Sepuluh Nopember, Surabaya, Jawa Timur, Indonesia

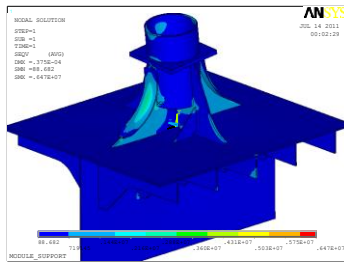*Corresponding author: jaswar@fkm.utm.my and jaswar.koto@gmail.com

Graphical abstract

Abstract

Floating Production Storage and Offloading (FPSO) in its operation is significantly affected by the environmental load as well as operational loads. These loads indirectly affect the structural components such as modules and its supports structures onboard of the FPSO. Investigation of fracture propagation has been carried out on the scantling support structure system of gas processing module. Modeling the structure with the finite element method (FEM) approach was performed by utilizing ANSYS 11.0 software. The fracture propagation evaluation is accomplished by elastic-plastic fracture mechanics with J-Integral method on crack first-mode (opening crack) accordance with DNV-OS-F201. As case study, FPSO Belanak operated at Conoco Block B in Natuna, Indonesia was investigated.

Keywords: Fracture; scantling support structure; processing module; FPSO; j-integral; sif; crack propagation

■1.0 INTRODUCTION

The concept of Floating Production Storage and Offloading (FPSO) is introduced to replace the system of fixed production platform with a floating storage facility or a Floating Storage Offloading (FSO). It should be noted, for shallow water production platforms can be a jacket or a jack-up, while in deep water can be a semisubmersible or TLP. FSO itself is a vehicle that serves as a terminal, dedicated to serving the storage of the processed oil and gas production platforms in the fields of operations, and transferred them to the tank carrier ships that periodically come.

The FPSO is basically a single hull ship functioned as a vehicle to accommodate the facilities on the deck in order to process the products as well as oil and store it in tanks in the side before the product is transferred to tankers transporting for distribution to the market.

On the deck of the FPSO there are various types of buildings according to their respective functions. As an example of topside building to support the production process is gas processing module. Weight of the topside modules and the load environment which is wave loads, significantly influence the strength of the deck that supports the FPSO. As topside module should be

supported with a strong support structure system, preventing the occurrence of fracture failure on the FPSO deck is required.

Current research takes a case study on the fracture propagation analysis of the scantling support system FPSO Belanak. FPSO Belanak operating in Indonesia Natuna waters was exactly at the Eastern Area of Conoco Block B.

■2.0 LITERATURE REVIEW

Study on fracture cause of failure in the ship structure has occurred since the early 1900s. S.T. Rolfe (1975) analyze comprehensively about the criteria of hardness (toughness) to the hull that can be used for steels with varying levels of strength. In fact the stress concentration always occurred in the construction of complex structures by welding, such as ships. Local high voltage resulted in a discontinuity or defect will occur in the hull (Rolfe, 1975).

Analysis of crack initiation and crack propagation in ship structures have been conducted since 1998 (Andersen, 1998). Ayyub and Souza (2000) analyzed the fatigue life of ship structures based on reliability. Analysis of ship structures experienced an increase. At the beginning of the study focused on

the behavior of crack initiation to failure, until in the present analysis of ship structures lead to structural reliability and risk in the event of failure of the structure.

Application of fracture studies with fracture mechanics of elastic plastic approach would be more appropriate to use to analyze the behavior of embedded cracks and deformation properties of the material has a larger plastic after accruing continuous loading of a material such as Ductile. As we know that the materials Ductile material is often used as the compiler of bed material of the building structure. Based on previous research done on the tubular structure (Aulia, 2005) crack propagation behavior has adapted to the analysis results presented by Broek (1987) analysis based on elastic plastic mechanics fracture. This method is suitable applied in the analysis fracture in offshore structure.

During its development, including three-dimensional crack straight through-crack, surface crack, corner crack and embedded crack studies have been carried out. The fact reveals that the embedded crack is more common in brittle and ductile materials having a catastrophic impact of hazards. Even though recent research using the theory of elastic plastic crack embedded resolution states that using these parameters, namely J, Q, and Tz is able to explain well the crack front with increasing radius and strain hardening exponent (Zhao, 2009). The same thing is also disclosed in an earlier study, that the approaches J, the relative can be used in a variety of purposes relating to fracture, taking into account the concept of stress-strain on the material (Dowling, 1987).

According to Barsom (1987), cracks have been investigated in several classes of tankers. Even though according to research by Wang (2009) of some material and the formulation of crack propagation, propagation behavior will be more clearly observed by including a load factor of the ratio of the work.

Kurniawan (2010) conducted the reliability analysis scantling support module to fatigue loads, the results of fatigue life of 116.3 years, or 3.88 times the lifespan of its operations. Ardhiansyah in 2010 also conducted the reliability analysis scantling support module against extreme loads, the combination of the three extreme loads obtained maximum stress 96 MPa and the obtained results of the structure remains safe to operate.

■3.0 WAVE LOAD

In the planning process offshore structure (offshore structure), the determination of the structure of work ability is influenced by the work load on the structure. Designer must determine the accuracy of the load to be applied in the planning of offshore structure in advance.

According to Indiyono (2003) wave load is the biggest load caused by environmental load on offshore structure. FPSO exposed to wave load will accelerate in every movement. Scantling support facility structure gas system processing module located on the FPSO is also accelerated due to the movement of the FPSO. In accordance with Newton's second law, the existing structures on the vessel will experience a force due to vessel movement resulting in acceleration. For translational motion, inertia force is obtained in Equation 1.

$$F = m \times a \tag{1}$$

where; m is mass and a is acceleration

According to Bhattacharayya (1978), there are four moments of rotational motion is important that inertial moment, damping moment, restoring moment, and exciting moments. Moment of inertia equation is:

$$I = mr^2 \tag{2}$$

where m is mass of the ship (kg), r is radius of gyration (m). Whereas for the moment force, the equation is:

$$Moment = I\alpha \tag{3}$$

where α is acceleration rotary (rad/s^2) and I is inertial moment (kg.m^2)

Response on offshore structures (either fixed or floating structure) due to regular waves in each frequency, can be determined by using spectra method. Response Amplitude Operator (RAO) or often referred to as the Transfer Function is a function of the response caused by the waves in the frequency range of offshore structures.

RAO is a tool for transferring force to the wave movement dynamic response of structures. According to Chakrabarti (2005), RAO equation can be searched with the following equation.

$$RAO(\omega) = \frac{X_p(\omega)}{\eta(\omega)} \tag{4}$$

where $X_p(\omega)$ is amplitude of the structure and $\eta(\omega)$ is amplitude of the wave

Response spectrum is multiplication between wave spectrum with RAO square. Equation from the response spectrum is (Chakrabarti, 1987) as follows:

$$S_R(\omega) = [RAO(\omega)]^2 \, s(\omega) \tag{5}$$

where $S_R(\omega)$ is response spectrum (m^2-sec), $s(\omega)$ is wave spectral (m^2-sec), RAO is Response amplitude operator, ω angular frequency (rad/sec).

■4.0 FRACTURE MECHANICS

Fracture mechanism initiated by the presence of cracks (crack) on the surface of the connection. This mechanism is the local conditions of stress and strain around the crack is influenced by global parameters such as loading, material properties, and geometry. Repeated loading (cyclical) will cause the crack to grow and lead to failure of the connection that eventually resulted in the failure of structure overall.

Methods of Linear Elastic Fracture Mechanic (LEFM) is a method that shows the relationship between stress field and its distribution around the crack tip with the size, shape, orientation of cracks, and material properties due to external load imposed on the material. Methods of Linear Elastic Fracture Mechanic (LEFM) can be used for very small plastic region, where the voltage is lower than the voltage of the license (σ <0.8 σ$_{ys}$) (Broek, 1987).

As linear elastic methods is inappropriate used in large structures using low-or moderate-strength steel for large plastic zone around the crack, thus causing the elastic-plastic behavior. It is developing methods elastic plastic fracture mechanics (EPFM) to show the characteristics of plastic material behavior.

J-integral is a contour in the region around the crack tip. The main concept is the energy balance between the stored strain energy and effort to work by external forces to explain the energy available for crack growth. J-integral is equivalent to force the growth of small cracks in the contours near the crack tip that considered.

Stress and strain field measurements on average are going on around the crack tip in elastic-plastic behavior, symbolized with J. A relationship J with K can be viewed at the following equation.

$$J = \frac{K_I^2}{E'} \tag{6}$$

where E' is E for plane stress and $E' = E / (1 - v^2)$ for plain strain. E is modulus Young and v is the Poisson ratio.

5.0 STRESS INTENSITY FACTOR

Stress intensity factor is a parameter that contains the concept of energy balance principle and the distribution around the crack tip. If the stress intensity factor (K) reaches the threshold stress intensity factor (K threshold), then the cracks began to spread, and failure of occurs when the price structure (K) has reached a critical material (KIC) that called fracture toughness.

In this study used the type of Center Crack in Finite Width Strip, can be seen from Figure 1. From the Figure 1, it know that the direction of crack propagation towards thickness or depth and the direction of circumferential that happening.
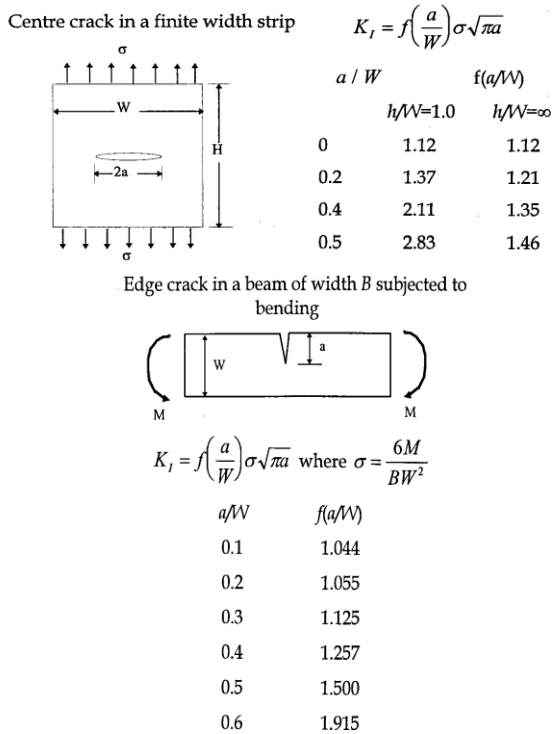

Figure 1 SIF on the type of center crack in finite width strip (Wang, 1996).

6.0 CRACK PROPAGATION

At fracture mechanics, the addition of crack size ($\Delta\alpha$) during one cycle of loading (load cycle) is related to the stress intensity factor range ΔK for the loading cycle. This relationship is expressed in the Paris and Erdogan formulation as follows (Almar-Naess, A. Ed, 1985):

$$\Delta\alpha = C(\Delta K)^m \tag{7}$$

The addition of cracks in one cycle is usually very small compared to the size of the cracks. So that Equation 7 can be written as follows (Anderson, 1998):

$$\frac{d\alpha}{dN} = C(\Delta K)^m \tag{8}$$

The existence of the mean stress causes the necessity of adding a correction factor to the Paris equation as modifications made Foreman, for EPFM method must be corrected with plastic so that the elastic parameters of Equation 8 becomes (Barsom, 1987):

$$\frac{d\alpha}{dN} = \frac{C(\Delta J)^m}{1-R} \tag{9}$$

where

$$\Delta J = \frac{\Delta K_I^2}{E'}$$

To get the number of cycles when there is a failure, then do the integration of Paris equation (Bai, 2003):

$$N_f = \int_{a_0}^{a_{cr}} \frac{d\alpha(1-R)}{C(\Delta J)^m}$$

$$N_f = \frac{a_{cr} - a_0(1-R)}{C\left(\frac{\Delta K_I^2}{E'}\right)^m} \tag{10}$$

7.0 SIMULATION AND DISCUSSION

7.1 Simulation Condition

A study of literature and data collection from books, textbook, journal, and discussion report which is similar to this study is included. In addition, the search was also conducted on the data FPSO Belanak include environmental data, ship structure and data scantling support structure. Figure 2 shows the distribution modules and location of the support structure which is investigated in this research.

Modeling FPSO was designed using Maxsurf to obtain the coordinates of the structure of the FPSO. Then convert the modeling conducted in Maxsurf to MOSES to get RAO. Performed loading of FPSO Belanak structures are used to find the reaction force of the global FPSO structures due to wave loads acting on the FPSO Belanak.

Validate the results of calculations with the data prior to this research. After getting the inertia force on the center of gravity module and the 8 legs support structure, performed stress analysis calculations (stress analysis) by modeling locally scantling support structure with ANSYS.11 to review the stress distribution on the support structure scantling.

Modeling of initial crack is assuming dimensions in accordance with DNV OS F201 code. Location of crack initiation is at the location of the hotspot stress that has been obtained from running the model with the structure of the actual load. After modeling the crack is done, the next step is to enter the maximum and minimum loading of the previous global analysis.In a two-component gel, it is easy to modify the molecular structure of either of the two components.
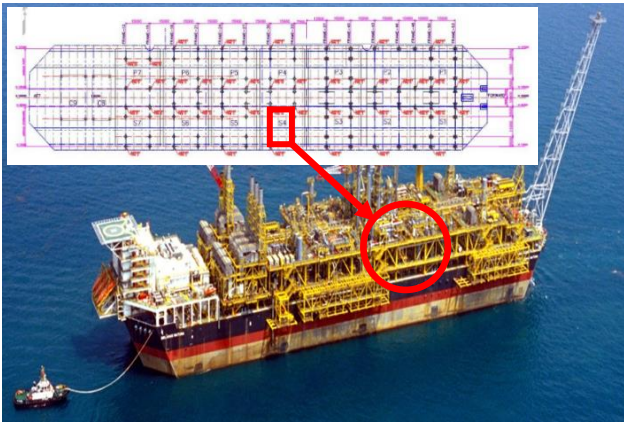
Figure 2 Location of support structure modules on the FPSO Belanak (McDermott, 2010)

7.2 Global Analysis

Results of simulation covers global analysis, local analysis, and crack propagation. Wave load calculation was performed to obtain single amplitude accelerations, wave drift force, and the Response Amplitude Operator (RAO) motion of the FPSO to the five-way wave heading which are the direction of 0º, 45º, 90º, 135º and 180º in surge motion, heave, sway, roll , pitch and yaw. The calculation is done on the condition of the Light Draft Vessel with draft 16.2m, with MOSES 6.0 software and wave conditions was 100 annual wave conditions.

The results of calculation of the maximum single-amplitude accelerations relative to the MOSES 6.0 with relative points are used there is 9 points that is reviewed, the module and support structure as much as 8. Here is an output of maximum single amplitude accelerations compared with data owned by Conoco Phillips as found in Table 1.

Table 1 Maximum single amplitude accelerations

| Comparison | Degree of Freedom (Max Acc) | | | | | |
	Surge	Sway in m/s²	Heave	Roll	Pitch in rad/s²	Yaw
Conoco Philips (2002)	0.656	2.180	1.054	3.023	0.679	0.193
Module	0.232	0.716	1.363	2.455	0.575	0.271
Leg 1	0.189	0.750	1.487	2.455	0.575	0.271
Leg 2	0.179	0.750	1.460	2.455	0.575	0.271
Leg 3	0.174	0.750	1.412	2.455	0.575	0.271
Leg 4	0.174	0.750	1.391	2.455	0.575	0.271
Leg 5	0.189	0.749	1.432	2.455	0.575	0.271
Leg 6	0.179	0.749	1.317	2.455	0.575	0.271
Leg 7	0.174	0.749	1.269	2.455	0.575	0.271
Leg 8	0.174	0.749	1.248	2.455	0.575	0.271

FPSO affected by wave loads will accelerate in every movement. Module facility located on the FPSO is also accelerated due to the FPSO motion, then according to Newton's law of accelerating objects that have a force. FPSO experience translational and rotational motion due to wave loads. For translational motion, inertia force is obtained by Equation 1. For the rotational motion, inertia force obtained with Equations 2-3.

Gas processing module FPSO Belanak has 8 support structures with configuration as shown in Figure 3. Distance of

the support structure closest to the center line FPSO is 5 m. While the size of the gas processing module itself is 22 x 30 m. Support Structure located on frame 30 and 33 of the FPSO. Therefore, the load response on each leg was calculated to determine its structure support that receives the most critical load.
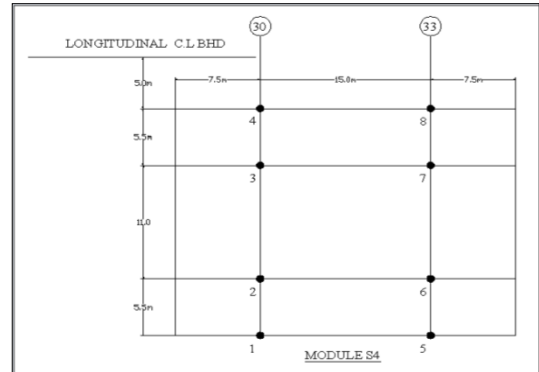

Figure 3 Configuration of support structure

With the distance mass points between the COG FPSO with mass points of each support structure different from each other. Between leg leg 1 through 8 will have a different reaction in receiving the load of motion FPSO itself. From the calculation results can be seen that the structure of support that receives the greatest load is on the leg 5 as shown in Figure 4.
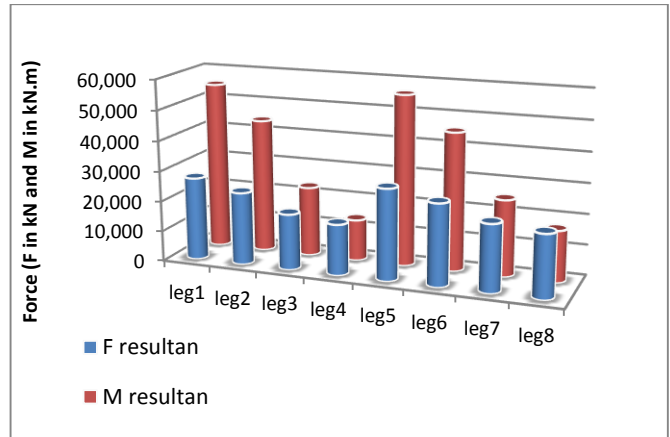

Figure 4 Load on the support structure

7.3 Local Analysis

In local analysis, the area taken is a connection part between ship hull with scantling support module. Local analysis phase performed using ANSYS.11 software with a focus on the scantling support structure of gas processing module. In the simulation, the scantling area is locked from movement in all directions, but the support structure is free movement in 6 degree of freedom (6-DOF) show on the Figure 5.

Figure 6 is a local model of scantling support structure that has been given a load, obtained from global analysis. The figure shows stress distribution around the connection between hull and scantling support module with stress of 6:47 MPa which is the largest stress value (hotspot stress) on the structure.
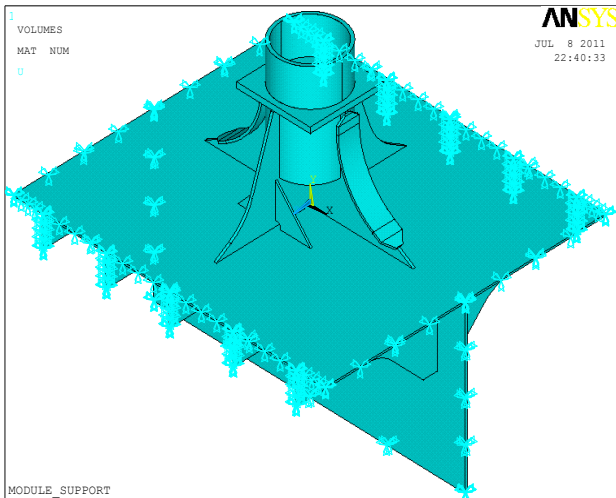
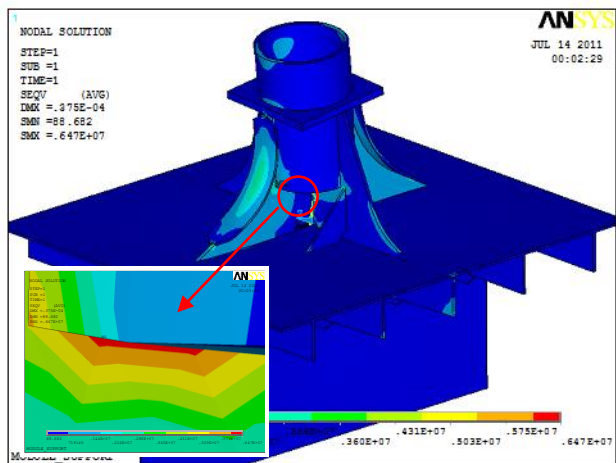**Figure 5** Local modeling of support structure in ANSYS 11

Figure 6 Stress distribution and hot spot stress

Figure 7 Initial crack

Figure 8 Stress distribution on initial crack

Given initial crack in this research are assuming dimensions in accordance with DNV OS F201 code. Location of crack initiation is at the location of the hotspot stress that has been obtained from running the model with structure of the actual load as shown in Figure 7.

After modeling the crack is done, the next step is to enter the maximum and minimum loading of the previous global analysis. In the simulation, the scantling area is locked from movement in all directions, but the support structure is free movement in 6 degree of freedom (6-DOF). Here are loading and the results of running ANSYS for the loading in the initial crack can be seen in Figure 8. From the results obtained for the highest stress 25.1 MPa.
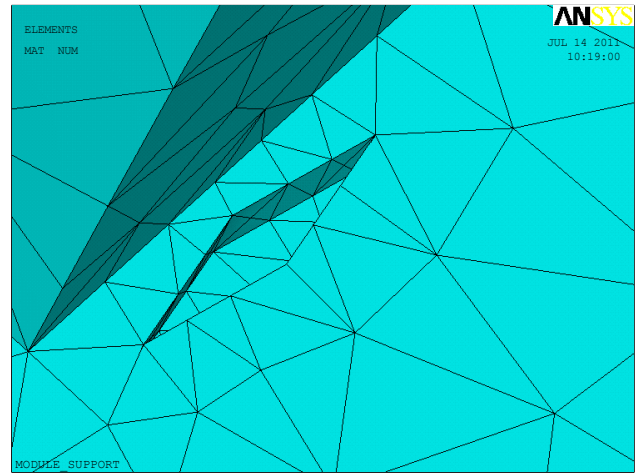
7.4 Crack Propagation
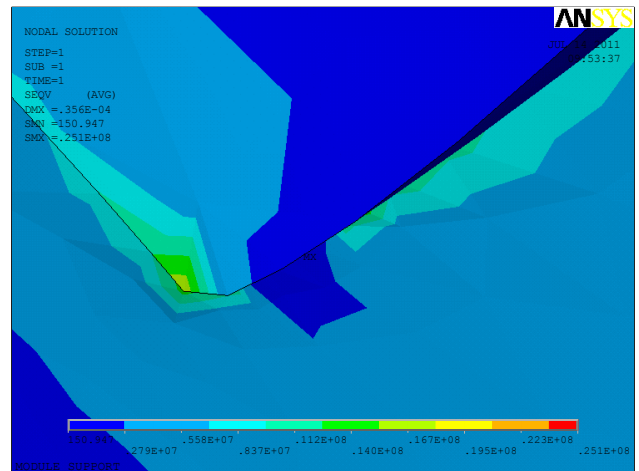
From the results obtained from the local analysis, obtained the maximum stress is at the tip of crack, according to the theory of embedded elliptical crack, which is when $\beta = \pi / 2$ and stress obtained by the Table 2.

Table 2 Output stress at the initial crack

			σ (Pa)		
	X	**Y**	**Z**	**Sint**	**Seqv**
Max	1.02E+07	2.25E+07	1.09E+07	7.81E+07	7.31E+07
Min	1.96E+06	1.45E+06	3.57E+05	1.07E+07	1.02E+07

Due to the Stress Intensity Factor Equation to be used only need to insert a stress perpendicular to crack propagation both the direction of thickness and the direction of circumferential, only the stress to the global Y axis ANSYS are used.

Stress Intensity factor is calculated in the 2 position that is the position of crack depth (thickness) and towards the circumference of the object (circumferential crack). Stress

Intensity factor circumferential direction calculated by the equation center crack in finite width strips on the equation at Figure 1. Stress Intensity Factor direction of thickness is also calculated by the equation at Figure 1. Stress Intensity Factor obtained in the direction of thickness (Kt) and direction of circumferential (Ks) in Table 3.

From Stress Intensity Factor calculations for the thickness direction of (Kt) and direction of circumferential (Ks), then look for the Stress Intensity Factor Range (ΔKI). ΔKI value has a value greater than the value ΔKth 0:11 MPa √ m, indicating the occurrence of crack propagation in the plate.

In this study, for calculations crack propagation performed on the direction of the thickness of the plate with a variation of the initial crack 0.0001 up to 0015. To calculate the rate of crack propagation, there should be a conversion value of the stress intensity factor into the value of J. The analytical value of J obtained by the concept of stress and strain field measurements of the average is going on around the crack tip using Equation 6. Figure 9 shows the variation of the difference in the value of ΔJ for various initial cracks. As shown in the graph, that ΔJ increases with increasing of the initial crack.

Table 3 Stress intensity factor of crack initiation

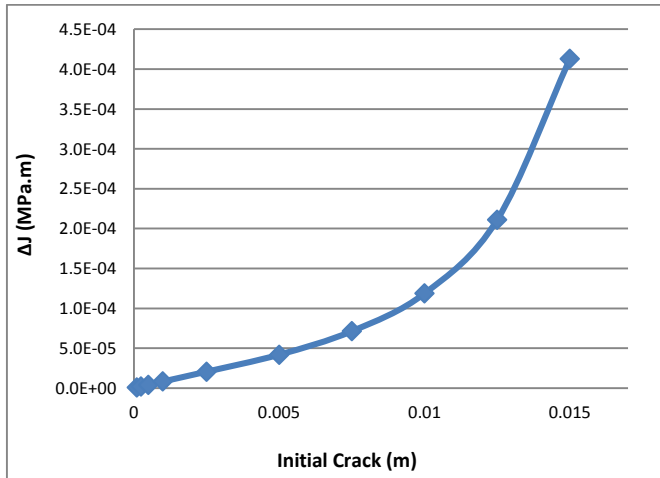|	**Circumferential Direction**				
	σ (MPa)	f(a/w)	√πa	K_I (MPa√m)	ΔK_I (MPa√m)
Max	2.25E+01	1.37	0.0886	2.73E+00	2.55E+00
Min	1.45E+00	1.37	0.0886	1.76E-01	
	Thickness Direction				
	σ (MPa)	f(a/w)	√πa	K_I (MPa√m)	ΔK_I (MPa√m)
Max	2.25E+01	1.055	0.01772	4.20E-01	3.93E-01
Min	1.45E+00	1.055	0.01772	2.71E-02	

Figure 9 Chart *ΔJ* to initial cracks

Crack propagation is the number of cycles with a given initial crack up to a certain size to happen next or crack propagation. Crack propagation is influenced by the magnitude of ΔJ. The larger ΔJ, the faster the propagation occurs.

The curves of crack propagation on crack initiation, can be seen in Figure 10. The curve below shows that the larger the initial crack, the greater the crack propagation.

Crack propagation is affected by ΔJ and ΔJ is influenced by the crack initiation. In this case the final propagation distance is assumed at 0.7 T, where T is the plate thickness. When the larger the value of crack propagation, the stress cycles (N) required to reach the critical crack will be larger.

From Figure 11 it can be seen that the larger the initial crack occurred, the smaller the number of cycles, with the understanding that the smaller the distance between the initial crack with a critical crack, the faster the rate of crack propagation.

By using the cycle from the calculation of crack propagation in the thickness direction (thickness), then look in the crack propagation circumferential direction. The results of the calculation of the crack propagation direction of circumferential crack propagation obtained largest occurred at 0.0084 mm. The results obtained have not yet reached the critical fracture rates. Value for critical crack circumferential direction is accordance to DNV OS F201 at 5 times the thickness direction of the critical crack, which is 3.5t or equal to 87.5 mm. The results of the calculations are shown in Figure 12
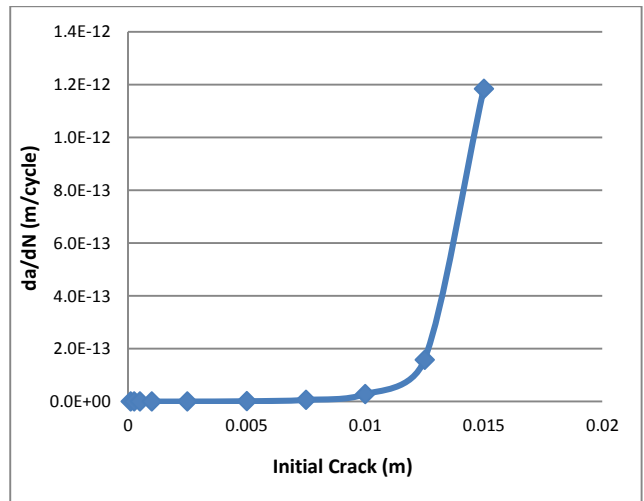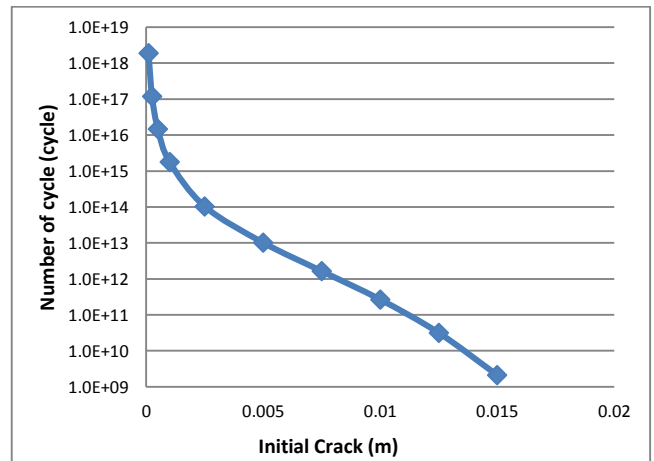

Figure 10 Crack propagation

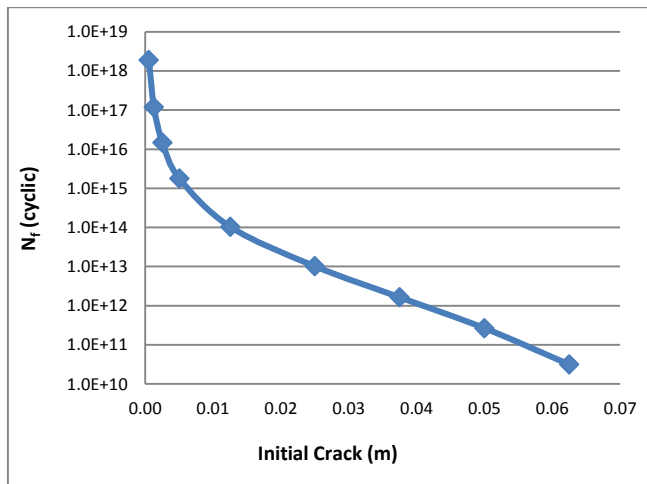**Figure 11** Number of cycles to initial crack

Figure 12 Crack propagation circumferential direction

■4.0 CONCLUSION

The conclusion to be drawn from this research is as follows:

1. Hotspot stress experienced by the Scantling support structure system gas processing module FPSO Belanak due to the loading is at 6:47 MPa and at initial crack conditions at 25.1 MPa which occurred in the scantling support structure system gas processing module.

2. Of providing the initial crack on the model of then obtained four values stress intensity factor, ie circumferential direction (K_s) maximum and minimum and thickness direction (K_t) maximum and minimum. Ks maximum value is equal to 2.73 MPa $\sqrt{}$ m and Ks is a minimum at 0176 MPa $\sqrt{}$ m. While the maximum value of Kt is equal to 0420 MPa $\sqrt{}$ m and minimum Kt is equal to 0.0271 MPa $\sqrt{}$ m.

3. That crack propagation occurs in the thickness direction (thickness) with a given variation in this analysis shows that the deeper crack initiation the faster rate of crack propagation. From the K values obtained and incorporated into the calculation of crack propagation thickness direction with the initial crack 0.1 mm up to the critical crack (0.7t or equal to 17.5mm), and the resulting number cycles at 1.89 x 1018 or 9.05 x 109 years. At the direction circumferential by the number of cycles 1.89 x 1018 was obtained crack propagation at 0.0084 mm.

Advice can be given from the results of the analysis in this research is:

1. Further analysis needs to be done with risk and reliability analysis approach.

2. In this research the location of cracks were found in the support module. Analysis needs to be done locally at the junction between the support brackets to the hull module.

In this study the load was reviewed is a wave load which produce inertia loads due to uncoupled motion. Needs to be done by considering the coupled motion analysis to determine the amount of the load inertia and crack propagation.

References

[1] Al-Obaid, Y. F. 1994. Automated Analysis of Topside Platform Hatch Covers Subject To Drill Collar Impact. PAAET. Kuwait.

[2] Almar-Naess, A.Ed. 1985. *Fatigue Handbook: Offshore Steel Structure.* Norway: Tapir Publisher.

[3] Andersen, M. R. 1998. Fatigue Crack Initiation and Growth in Ship Structure. *Thesis Department of Naval Architecht and Offshore Engineering*. Denmark: Technical University of Denmark.

[4] Ardhiansyah, Fahmy. 2010. Analisis Keandalan Scantling Support Structure System Gas Processing Module FPSO Belanak Terhadap Beban Ekstrem. *Tugas Akhir Jurusan Teknik Kelautan*. ITS. Surabaya.

[5] Aulia, S. 2005. Analisa Umur Kelelahan Turbular Joint Tipe T dengan Retak Eliptis pada Chord Menggunakan Metode Elastic Plastic Fracture Mechanics. Tugas Akhir: Jurusan Teknik Kelautan.

[6] Barltrop, N., Okan, B. 2000. FPSO Bow Damage in Steep Waves. Rogue waves 2000 workshop. Brest.

[7] Barsom, John M. & Rolfe,.Stanley T. 1987. Fracture and Fatigue Control in Structures. *Application of Fracture Mechanics*. New Jersey.

[8] Battacharyya, R. 1978. *Dynamic of Marine Vehicles*. John Wiley and Sons Inc. New York.

[9] Broek, David. 1987. *Elementary Engineering Fracture Mechanics*. Netherlands: Martinus Nijhoff Publishers.

[10] Broek, David. 1988. *The Practical Use of Fracture Mechanics*. Netherlands: Kluwer Academic Publishers.

[11] Bunce, J. W. 1977. Analysis of The Interaction Between The Module Structures and The Deck of an Offshore Oil Production Platform. Pergamon Ltd., Great Britain.

[12] Cameron, J. *et al.* 1997. Ultimate Strength Analysis of Inland Tank Barges. USCG Marine Safety Center.

[13] Chakrabarti, S. K. 2005. *Handbook of Offshore Engineering Volume I.* Offshore Structure Analysis Inc. Planfield. Illinois. USA.

[14] DnV Recommended Practice C205. 2007. Environmental Loads and Environmental Condition. Norway.

[15] DnV Recommended Practice OS-F201. 2001. Dynamics Risers. Norway.

[16] Dowling, N. E. 1987. J-Integral Estimates for Crack in Infinites Bodies. *Engineering Fracture Mechanic Journal*. 26(3): 333–348.

[17] Indiyono, P. 2003. *Hidrodinamika Bangunan Lepas Pantai*. Surabaya: Penerbit SIC.

[18] Kurniawan, Andri. 2010. Analisa Keandalan Scantling Support Structure System Gas Processing Module FPSO Belanak Terhadap Beban Kelelahan. Tugas Akhir Jurusan Teknik Kelautan. ITS. Surabaya.

[19] McDermott, J. 2010. Belanak FPSO Topsides Construction and Integration. OCEANO 2010 Seminar, 22th February 2010, ITS Surabaya, Indonesia.

[20] Nguyen, T. D. 2009. *Scantling Optimazition Ropax Ship*. University of Liege.

[21] O'Brein, D. P *et al.* 1993. *Recent Developments in Offshore Rig/Platform Evacuation*. Memorial University of Newfoundland. Canada.

[22] Palmer, A. C. 1997. *Breakup of Firewall Between The B and C Modules of Piper Alpha Platform-I. Analysis by Hand Calculation*. University of Cambridge. UK.

[23] Perez, Nestor.2004. *Elementary Engineering Fracture Mechanics*. Boston: Kluwer Academic Publishers.

[24] Rolfe, S. T. 1975. Fracture Mechanics, Fracture Criteria and Fracture Control for Welded Steel Ship Hulls. Prosiding Ship Structure Symposium.

[25] Shetty, N. K. *et al.* 1998. *Fire Safety Assessment and Optimal Design of Passive Fire Protection for Offshore Structures.* Elsevier Science Limited. Northern Ireland.

[26] UKOOA. 2002. Buckling and Ultinmate Strength Assessment for Offshore Structures. Glasgow.

[27] Wang, C.H. 1996. Introduction to Fracture Mechanics. DSTO Aeronautical and Maritime Research Laboratory, Melbourne

[28] Windergen, K V. 1994. Course and Strength of Accidental Explosions on Offshore Installations. Christian Michelsen Research. Norway.

[29] Zhao, J. 2009. Three Parameter Approach for Elastic-Plastic Stress Field of an Embedded Elliptical Crack. *Engineering Fracture Mechanic Journal*. 76: 2429–2444.